ELSEVIER

Chemical Engineering Journal 77 (2000) 99–104

Chemical Engineering Journal

www.elsevier.com/locate/cej

Tomographic imaging of transient multiphase flow in bubble columns

D. Schmitz, D. Mewes *

Institute for Process Engineering, University of Hannover, Callinstrasse 36, 30167 Hannover, Germany

Abstract

Vessels filled with liquid mixtures under high pressure and at high temperatures are used in many chemical processes. In the case of a process-breakdown, a sudden decrease of the pressure can occur. As a result, the liquid level inside the vessel swells and a blowdown of liquid and gas from the vessel occurs. For the operation of the plant, the design of the apparatus has to be safe and has to avoid similar states of operation. Therefore, the hydrodynamic phenomena occurring inside the vessel during the blowdown have to be known. Using electrical tomography it is possible to measure the distribution of the void fraction in each cross section of the vessel during the blowdown operation.

Keywords: Electrical tomography; Bubble columns; Pressure relief

1. Introduction

In recent years the standards for the chemical industry regarding safety, environmental protection, energy consumption, quality assurance and complexity of the products have increased significantly necessitating more complex and detailed measurement techniques for the design and control of chemical plants and transportation systems. During this development, the use of tomographic measurement techniques has become increasingly popular. The advantage of tomographic measurements in contrast to local measurements is the non intrusive imaging of the complete cross sectional area of the measured object once at a time. This is in contrast to local probes, which provide only local information. Since single probes, like one-point conductivity probes have been used by e.g., Menzel [1] or resistivity probes have been used by e.g. Idogawa et. al. [2] for the measurement of the radial void distribution in bubble columns.

The application of tomographic measurement techniques for process or chemical engineering applications is, in comparison to the medical sector, relatively new. Widely spread is the use of electrical, X-ray or NMR tomographic techniques.

The advantage of X-ray tomography is its high spatial resolution. The time resolution varies depending on the used sensor system. Very fast and expensive systems can reach measurement times of 0.5 ms with a spatial resolution of 2 mm [3]. Most of the used systems have imaging times of several seconds or minutes and are, therefore, not applicable for investigations on instationary multiphase flows. Kumar et al. [4] are doing measurements of the gas-hold up in bubble columns. Toye et al. [5] investigate stationary flows in trickle bed reactors, measuring the liquid distribution on the packing. Sederman et al. [6] are using NMR for the imaging of the pore structure within packed beds. With the NMR technique the fields of density and velocity are measured simultaneously. The technique is restricted to non-metal materials due to the magnetic field used for the measurements. Hence this technique cannot be used for pressure vessels.

Electrical capacitance tomography (ECT) is used for the investigation of pulsing flow in trickle bed reactors by Reinecke et al. [7]. Three phase flow was investigated by Johansen [8] using mixtures of oil, water and gas. The results of Xie et. al. [9] are dealing with horizontal plug-flow. The time resolution for in these applications are in the range of 100 frames per second. The spatial resolution depending on the diameter of the pipe is about 10% of the cross sectional area. The tomographic measurement technique presented in this paper combines a high measurement frequency with a high spatial resolution.

2. Experimental set-up

Fig. 1 gives the flow sheet of experimental set up. It consists of two pressure vessels (V1, V2), which can be operated with pressures up to 1.6 MPa. They are built of stainless steel and are tempered by a double shell. For the experimental investigations the temperature is set to 10°C and the pres-

* Corresponding author.
E-mail address: dms@c36.uni-hannover.de (D. Mewes).

1385-8947/00/$ – see front matter
PII: S1385-8947(99)00130-8

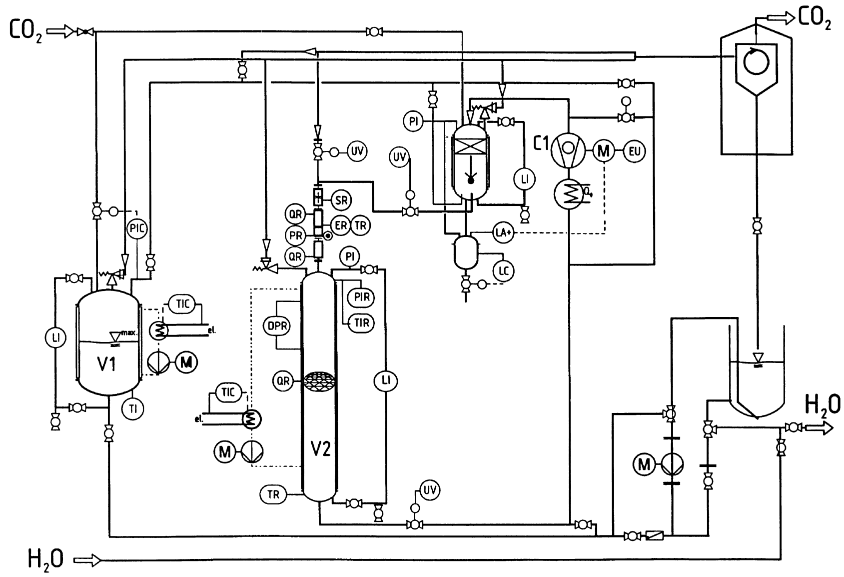

Fig. 1. Flow sheet of the experimental set-up.

sure to 0.9 MPa. In the first vessel V1, which has a volume of 300 l, tap water is saturated with carbon-dioxide. This is done by the carbon-dioxide circulation. Carbon-dioxide is taken from the top of the vessel, separated from the liquid by a separator and then compressed by the compressor C1. At the bottom of the vessel the gas is dispersed in the liquid phase. Due to the volume reduction the pressure inside the vessel is decreasing. To keep the pressure constant, carbon-dioxide is injected by a control loop. The liquid is saturated with carbon-dioxide. By weighing the carbon-dioxide supply bottle, the solved gas can be calculated.

In the next step the saturated liquid is pumped into the second vessel V2 which is shown in Fig. 2. This vessel is

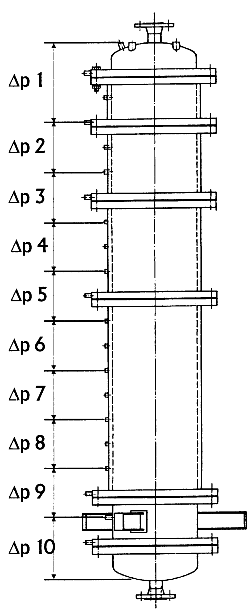

Fig. 2. Technical drawing of vessel V2.

2100 mm in height, and 315 mm in diameter has a volume of 160 l. It is built from five cylindrical segments of different length. The tomographic sensor is built in the vessel at different heights.

In addition to the tomographic measurement of the void fraction, the axial profile of the gas holdup is measured by 10 differential pressure transducers mounted in equal distances from the bottom to the top of the column. The void fractions measured by the differential pressure transducers are compared to the void fractions measured by tomographic sensor.

The blowdown is started by opening the ball valve at the top of the vessel V2. The pressure in the vessel V2 decreases rapidly and the liquid starts bubbling. The surface of the liquid rises and reaches the top of the vessel. A two-phase flow through the blow-off pipe is established. It takes about 1 min until the pressure reaches the ambient pressure. The time varies, depending on the viscosity and the level of the liquid at the beginning of the depressurization. The two-phase flow is separated at the end of the blow-off pipe by a cyclone separator.

In addition to the void fractions the temperatures at the top and the bottom as well as the pressures at the top of the vessel are measured.

In a second experiment the ball valve at the top of the vessel is controlled by one of the differential pressure transducers to avoid the two-phase flow in the vent-line. As a result the liquid remains in the vessel. The control-loop is given in Fig. 3. If the two-phase flow reaches the maximum level in the vessel the ball valve is closed again. The pressure in the vessel increases again and the two-phase flow mixture collapses. The ball valve is opened again when the two-phase flow mixture reaches the lower limit of the control mechanism. This is repeated until the pressure in the vessel reaches the ambient pressure.

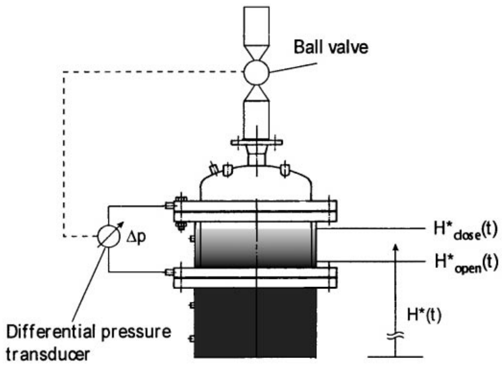

Fig. 3. Control of the ballvalve.

3. Tomographic measurement technique

For the measurement of the local void fractions a conductive tomographic measurement technique is used, that provides a spatial resolution of 5.3 mm and a time resolution of 100 measurements per second. The tomographic sensor consists, as depicted in Fig. 4, of three planes of parallel wires with an axial distance of 7 mm. The inner diameter is set to 315 mm, which is equivalent to the vessel diameter. The sensor is made of stainless steel coated with plastics for electrical isolation. It is constructed for a maximum pressure of 1.6 MPa. The sensor elements are sealed with carbon gaskets. This allows a disassembly of the sensor in the case of any repair of the wires. The wires are made of stainless steel with a diameter of 0.18 mm and are spaced 5.3 mm to each other. In that way in every plane 59 wires are stretched across the sensor, resulting in 58 integral measurement values. The individual planes are rotated 120° to each other in such a way that 4722 isosceles triangles are obtained. Between two adjacent wires in one plane the conductance is measured, which is direct proportional to the void fraction in the area covered by the wires.

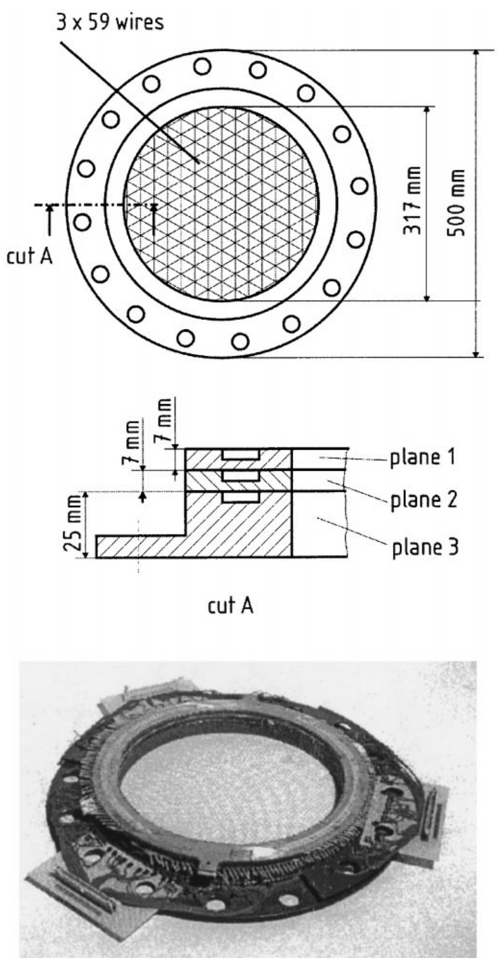

Fig. 4. Technical drawing and depiction of the tomographic sensor.

From the measured conductance the void fraction of each triangle is calculated by using the ART-algorithm. The computation is performed in an adapted coordinate system, as suggested by Reinecke et al. [10]. Details of the measurement technique are described by Reinecke et. al. [11].

3.1. Measurement accuracy

The accuracy of the measurements taken by the tomographic sensor is verified in a separate test loop. It consists of a vertical acrylic pipe with an inner diameter of 123 mm and 2.5 m in length. A second tomographic sensor of the same wire spacing is built into the test section at a height of 1.3 m. This smaller sensor is built with 3×21 wires resulting in 60 integral measurement values and 522 reconstruction elements. The impact of the wires on the void distribution and the measurement accuracy is investigated in a test loop by stationary bubbly flow. The gas flow rates are measured by a rotameter and are adjusted to superficial gas velocities up to j_g=0.3 m/s to cover the flow regimes from bubble flow to churn turbulent flow.

The bubbles are generated by using a perforated plate distributor. The distributor is made out of a Perspex-plate with a thickness of 3 mm. In the plate 121 holes with a diameter of 1 mm are arranged on six concentric circles. In all investigations the static liquid height to diameter ratio was set above eight, so that the bed height had negligible influence on the flow regimes. The void fractions and the bed expansion are measured by the tomographic sensors. In Table 1 the obtained volumetric void fraction $\varepsilon_g=(V_c-V_l)/V_c$

Table 1
Validation of the measured void fraction

j_g (m/s)	Tomographic sensor	Bed expansion
	ε_g	ε_g
0.016	0.024	0.024
0.026	0.051	0.04
0.052	0.11	0.09
0.12	0.19	0.15
0.18	0.24	0.18
0.27	0.23	0.24

for both measurements are given. The maximum deviation of the measured void fraction is about 25%.

By visual observation it was recognized that the flow is not effected by the sensor. This has also been confirmed by comparing the volumetric void fraction of the three measurement planes. If bubbles are caught in any of the planes, the measured average gas holdups of the three planes would be different. This has not been observed during the experimental investigations.

4. Experimental results

In Fig. 5 the pressure at the top of the vessel is plotted as a function of time for each initial liquid level in the vessel. The pressure decreases faster if the liquid level is higher at the beginning of the depressurization. In all blowdown experiments a first minimum of the pressure occurs within the first 5 s. After the desolve retardation time of the carbon-dioxide the oversaturated liquid starts to swell. This results in an increase of the pressure in the vessel and finally in a two-phase flow through the relief valve.

The tomographic sensor is located between the connections of the fifth differential pressure transducer connected to the vessel at 1052 mm.

In order to test the measurement accuracy of the tomographic sensor the measured void fractions are compared to the void fractions measured by the differential pressure transducers. In Fig. 6 both measurements are plotted as a function of time. The measured values match each other qualitatively as well as quantitatively. The increase in the volumetric gas-holdup after 2 s corresponds with the pressure minimum inside the vessel. The gas holdup reaches approximately 20% and is constant for the next 7 s. The maximum gas-holdup of 30% is reached after 16 s.

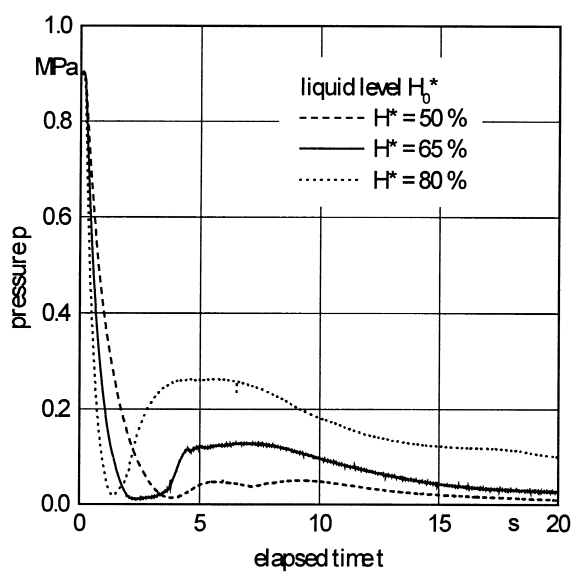

Fig. 5. Pressure at the top of the column as a function of time.

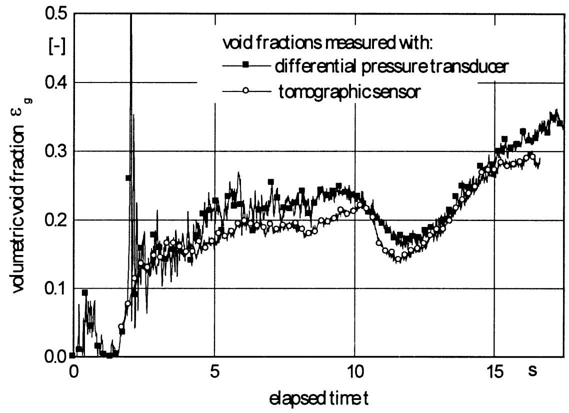

Fig. 6. Comparison of the volumetric void fraction measured with the differential pressure transducer and the tomographic sensor.

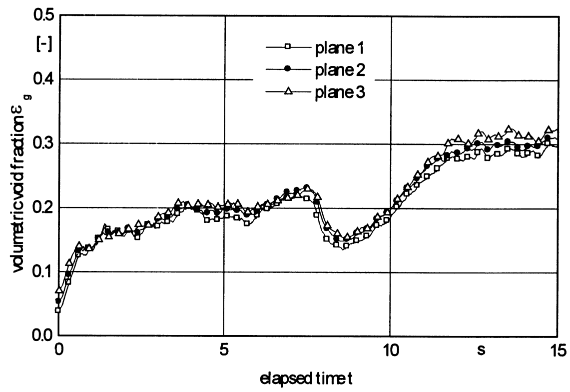

Fig. 7. Comparison of the volumetric void fraction measure in three different measurement planes.

In Fig. 7 the integral volumetric void fraction for each of the three measured cross sections is given. The results for all void fractions measured agree closely. This confirms the assumption that the wires of the sensor have no influence on the two-phase flow.

The void fraction distribution in the cross sectional area of the column from the tomographic measurements is shown in Fig. 8. On the left side the integral measurement values of

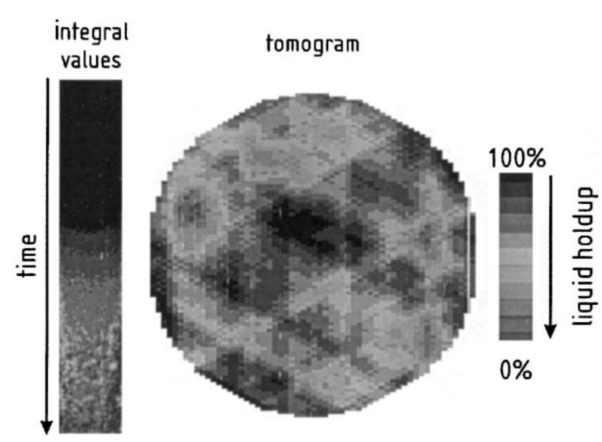

Fig. 8. Result of the tomographic recon-struction.

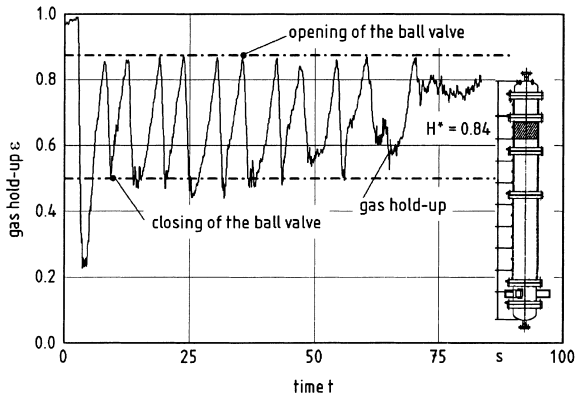

Fig. 9. Gas holdup as function of time for the control loop of the ball valve.

each projection is shown. The void fraction is scaled according to the table on the right side. The time scale starts at the top. The measurement frequency is 100 frames per second. Beside the results from the integral measurements, a tomogram is given at the right side. The tomogram is measured approximately 8 s after the starting of the blowdown. The level of the liquid is located at beginning of the blowdown at 65% of the vessel height.

After 2.5 s the carbon-dioxide starts to desorp, as indicated by the change of the colors from black to gray. First the gas-holdup rises at the wall of the vessel. The bubbles are generated at the wall due to the coarse surface. By selective undercooling of the wall section, the production of bubble nucleii can be reduced. Areas with a high gas-holdup can be distinguished from those with a low gas-holdup.

To avoid two-phase flow through the ventline, a controlled pressure relief is executed. As described above, the ball valve is controlled by one of the differential pressure transducers. In Fig. 9 the gas holdup measured with the second pressure transducer is given. At the beginning of the measurement the ball valve is opened and the liquid level rises. As the gas hold

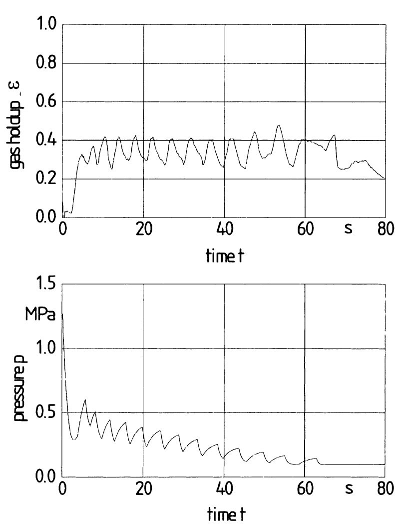

Fig. 10. Gas holdup and pressure as a function of time.

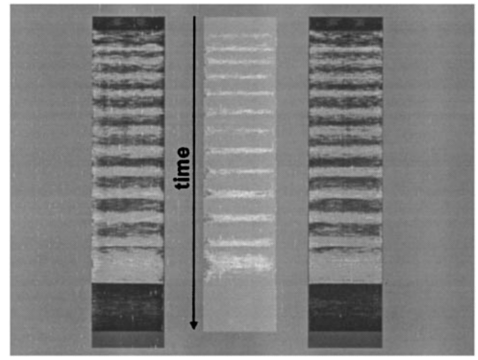

Fig. 11. Three-dimensional representation of the tomographic measurement.

holdup reaches the lower limit the ball valve is closed again. The gas holdup increases due to the rising pressure and the separating of the gas and the liquid in the column. With this control mechanism the liquid remains in the vessel. In Fig. 10 the gas holdup as well as the pressure in the vessel is given as a function of time. The gas holdup is measured with the tomographic sensor. During the experiment the ball valve is opened and closed sequentially which results in the given pressure curve. The ball valve is closed 13 times in total. The time of the controlled pressure relief is with approximately 70 s equivalent to the time for the continuous pressure relief. The gas holdup during the experiment oscillates between 25 and 40%.

In Fig. 11 the result of the tomographic measurement is given as a three-dimensional picture. The time starts at the top of the picture. In the middle of the picture an isosurface of the gas holdup is given. In addition two orthogonal slices are shown. In each slice the changes of the gas holdup during the pressure relief are visible.

5. Conclusions

Electrical tomography can be applied for the measurement of the phase distribution during the blowdown of a pressurized vessel. Due to the high time resolution it is possible to measure the alteration of the void fraction during the pressure relief process. The sensor is mounted at different axial positions in the column in order to get the void fraction distribution in the axial direction. The experimental data is useful for further numerical modeling of the blowdown process.

Acknowledgements

The authors wish to thank the German Research Foundation (DFG) for financial support.

References

[1] T. Menzel, Die Reynolds-Schubspannung als wesentlicher Parameter zur Modellierung der Strömungsstruktur in Blasensäulen und Airlift-Schlaufenreaktoren, Düsseldorf, VDI-Verl., 1990.

[2] K. Idogawa, K. Ikeda, T. Fukuda, S. Morooka, Behavior of bubbles of the air-water system in a column under high pressure, Int. Chem. Eng. 26 (3) (1986) 468–474.
[3] K. Hori, T. Fujimoto, K. Kawaniski, H. Nishikawa, Advanced High Speed X-ray CT Scanner for Measurements and Visualization of Multiphase Flow, OECD/CSNI Specialist Meeting, Santa Barbara, USA, 1997.
[4] S.B. Kumar, D. Moslemian, M.P. Dudukovic, Gas-holdup measurements in bubble columns using computed tomography, AIChE J. 43 (6) (1997) 1414–1425.
[5] D. Toye, P. Marchot, M. Crine, E. L'Homme, The use of large scale computer assisted tomography for the study of hydrodynamics in trickling filters, Chem. Eng. Sci. 49 (24b) (1994) 5271–5280.
[6] A.J. Sederman, M.L. Johns, A.S. Bramley, P. Alexander, L.F. Gladden, Magnetic resonance imaging of liquid flow and pore structure within packed beds, Chem. Eng. Sci. 52 (17) (1997) 2239–2250.
[7] N. Reinecke, D. Mewes, Tomographic imaging of trickle-bed reactors, Chem. Eng. Sci. 51 (10) (1991) 2131–2138.
[8] G.A. Johansen, T. Frøstein, B.T. Hjertaker, O. Olsen, A dual sensor flow imaging tomographic system, Meas. Sci. Technol. 7 (3) (1996) 297–307.
[9] C.M. Xie, A. Plaskowski, M.S. Beck, 8-Electrode capacitance system for two-component flow identification, Part I: tomographic flow imaging, IEEE Proc. 136 (4) (1989) 173–183.
[10] N. Reinecke, G. Petritsch, D. Mewes, Reconstruction of limited view problems by using adapted coordinates, in: Proceedings of the Meeting on Fluid Engineering Division Summer Meeting, Vancouver, 1997.
[11] N. Reinecke, M. Boddem, D. Petritsch, D. Mewes, Tomographic imaging of the phase distribution in two phase slug flow, Int. J. Multiphase Flow 24 (4) (1998) 617–634.